All-Optical Wavelength Conversion Using a Pulse Reformatting Optical Filter

Juerg Leuthold, *Member, IEEE*, Dan M. Marom, Steven Cabot, James J. Jaques, Roland Ryf, and C. Randy Giles, *Fellow, OSA*

***Abstract*—We introduce a general concept for the design of all-optical wavelength converters with pulse reformatting functionality. The novel wavelength converters are based on a single semiconductor optical amplifier followed by an optical filter. A microelectromechanical system-based realization is shown and simultaneous 40 Gb/s wavelength conversion, switching and signal format conversion is demonstrated. The new pulse reformatting optical filter device outperforms current schemes with respect to input-power requirements, input-power dynamic range and signal quality.**

***Index Terms*—All-optical, all-optical routing, semiconductor optical amplifier, spectral processing, wavelength conversion.**

I. Introduction

LOW INPUT-power all-optical wavelength converters (AOWCs) offering not only protocol but also bit-rate transparency are of high interest for future networks. They may replace expensive, power and space consuming optical-to-electrical-to-optical (OEO) converters used to overcome wavelength blocking issues and they may be needed for performing signal regeneration.

AOWCs exploiting semiconductor optical amplifier (SOA) nonlinearities in interferometric configurations [1]–[18] have already demonstrated operation up to 160 Gb/s [1] and pattern independent operation up to 100 Gb/s [2]. In addition to high speed they have shown 2R (reamplification, reshaping) [3]–[8] and 3R (reamplification, reshaping and retiming) regenerative capabilities [9], [10] with broadband performance over as much as 80 nm [11].

Many implementations of all-optical wavelength conversion schemes have been proposed and discussed in the literature. Interferometric configurations, such as the Mach-Zehnder interferometer (MZI) configuration [12], [13], the Terahertz Optical Add-Drop Multiplexer (TOAD) [14], the ultrafast nonlinear interferometer (UNI) [15], [16] and the differential delay interferometer (DI) configuration [17], [18], exploiting the cross-phase modulation (XPM) effect have received considerable attention due to the low input-power requirements and operation in a differential mode enabling speeds beyond the SOA carrier recovery times [13], [20].

Recently, novel schemes have appeared that no longer solely exploit XPM in a differential scheme. For instance, a gating method for the delay interferometer configuration has been introduced [21]. With this method both pattern independent 100 Gb/s operation [2] as well as successful 1 000 000 km 3R transmission were demonstrated [10]. The method relies on both cross-phase and cross-gain modulation and has an ideal operation speed that is approximately twice the operation speed of a conventional SOA carrier recovery time limited system [22]. Recently, successful WDM 2R transmission over 16 800 km was demonstrated with a red-shift optical filtering (RSOF) scheme [8]. These two schemes and the aforementioned differential delay interferometer scheme employ a common configuration based on a single nonlinear section followed by an optical filter.

In this paper, we report a general concept for the design of all-optical wavelength converters and regenerators. Our configuration is a single SOA followed by a pulse reformatting optical filter (PROF). The scheme explicitly takes into account both SOA cross-phase and cross-gain modulation effects. It provides within first order—what we believe—the best possible conversion efficiency for an SOA-based wavelength converter or regenerator. These findings are supported by experiments demonstrating 40 Gb/s all-optical wavelength conversion with as little as -17.5 dBm input signal powers and a dynamic input power range of as much as 11–20 dB. The current realization of a PROF filter is based on MEMS technology. Advantages of this PROF implementation are as follows.

- Simultaneous all-optical wavelength conversion, switching, power equalization and output format conversion.
- Multiwavelength conversion of WDM signals in a single filter similar to our earlier RSOF scheme [8].
- Transparency to bit-rates as long as the filter has the resolution and passband for both lower and higher speed and the speed limitation of the nonlinear element is not exceeded.
- Low input power and large input power dynamic range making additional amplification of a single channel within the switch fabric unnecessary.
- Further, it shares the many advantages of other pattern independent all-optical wavelength conversion schemes which provide transparency to protocols and in particular to protocols that favor bursty traffic.

II. Theory and Operation Principle

The new all-optical wavelength converter comprises an SOA and a pulse reformatting optical filter schematically shown in Fig. 1.

For all-optical wavelength conversion the input data signal P_{in} and the cw light P_{cw} are launched into the SOA. In the SOA

Manuscript received July 15, 2003; revised October 14, 2003.

The authors are with Bell-Labs, Lucent Technologies, Holmdel, NJ 07733 USA (e-mail: Leuthold@Lucent.com).

Digital Object Identifier 10.1109/JLT.2003.822158

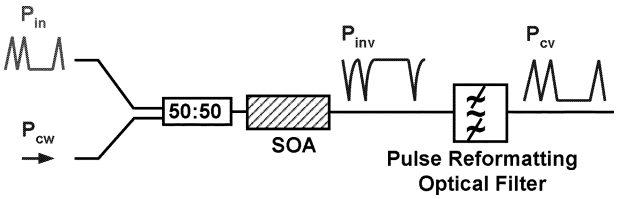

Fig. 1. Input signal $P_{\rm in}$ is guided into an SOA thereby modulating the SOA carriers. The carrier depletion in the SOA affects the cw signal by means of cross-gain and cross phase modulation producing an inverted signal $P_{\rm inv}$ at the cw frequency. A filter then reformats the $P_{\rm inv}$ signal into an output signal with the desired pulse shape of $P_{\rm cv}$.

the input data signal encodes the signal information by means of cross-gain and cross-phase modulation onto the cw signal. As a result we obtain at the SOA output a chirped and inverted signal $P_{\rm inv}$ at the wavelength of the cw light. The purpose of the subsequent passive optical filter with an appropriate amplitude and temporal response is to reformat the signal $P_{\rm inv}$ into a new output-signal $P_{\rm cv}$ with a determined shape.

The ideal frequency response of the pulse reformatting optical filter that transforms the inverted signal $P_{\rm inv}$ into the desired output signal $P_{\rm cv}$ can be calculated by applying optical filter theory [23]. Accordingly, the frequency response of the output signal $H_{\rm cv}(\omega)$ needs to be divided by the frequency spectrum of the input signal $H_{\rm inv}(\omega)$, to obtain the complex frequency response of the PROF filter

$$H_{\rm PROF}(\omega) = \frac{H_{\rm cv}(\omega)}{H_{\rm inv}(\omega)}. \tag{1}$$

The frequency response $H_{\rm PROF}(\omega)$ of the PROF filter can be calculated if both the desired temporal response of the converted signal at the output and the inverted signal behind the SOA are known and well defined. In practice we need the amplitude transfer function and the group delay of the corresponding filter. The amplitude transfer function is the absolute value of $H_{\rm PROF}(\omega)$ and the group delay is given by

$$\tau_g(\omega) = \frac{-1}{2\pi}\frac{\partial}{\partial\omega}\tan^{-1}\left(\frac{\mathrm{Im}\left(H_{\rm PROF}(\omega)\right)}{\mathrm{Re}\left(H_{\rm PROF}(\omega)\right)}\right). \tag{2}$$

A. RZ to RZ All-Optical Wavelength Conversion

In order to find the PROF filter for performing RZ to RZ wavelength conversion we need the frequency spectra of both the converted signal and the inverted signal after the SOA. We are interested in generating a Gaussian shaped converted output signal with a FWHM of ~6 ps (this is an arbitrary choice—other FWHMs can be chosen), corresponding to a Gaussian frequency spectrum for $H_{\rm cv}(\omega)$. To obtain an accurate frequency spectrum of the inverted signal behind the SOA we experimentally measure the time response $P_{\rm inv}(t)$ and phase response $f_{\rm inv}(t)$ and use this information to calculate the frequency response $H_{\rm inv}(\omega)$. The signal shape and frequency spectrum of these signals are depicted in Fig. 2. Applying (1) and (2) we find the amplitude transmission and group delay response of the ideal filter depicted at the bottom of Fig. 2 (solid lines). In order to make

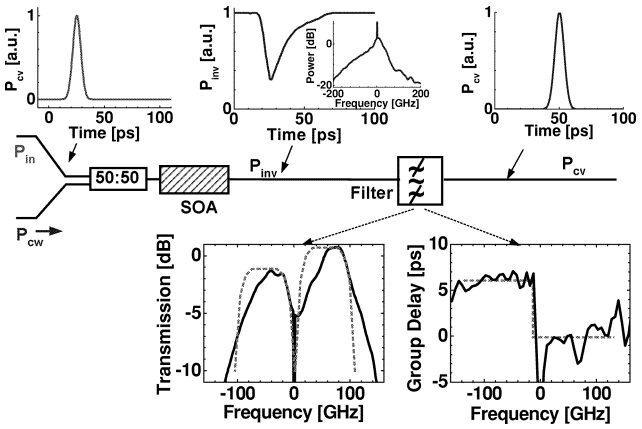

Fig. 2. All-optical wavelength converter comprising an SOA and a pulse reformatting optical filter (PROF). In this scheme, the input signal $\mathrm{P_{in}}$ is mapped by means of SOA cross-gain and cross-phase modulation into an inverted pulse $\mathrm{P_{inv}}$ at the cw wavelength. The transmission and group delay of the ideal PROF that reformats the $\mathrm{P_{inv}}$ into a Gaussian signal are shown in the bottom insets (solid lines). The dashed lines show a three-segment approximation to this filter. All frequency offsets are given with respect to the cw center frequency.

such a filter practical we have approximated this ideal filter by means of a step filter as depicted by the dashed lines. In this approximation we cut the frequency spectrum into three spectral slices and introduce an individual attenuation and group delay to each of the spectral slices before recombining them into a single signal. Our simulations and experiments show that this approximation is sufficient to provide converted signals of excellent signal quality. The spikes in the group delay plot are due to small fluctuations in our experimentally measured inverted signal. They would average out if more measurements were done.

The PROF filter concept can be understood intuitively by means of mode beating. To gain physical insight we first discuss the time and frequency response of the cw signal $P_{\rm inv}$ after an input signal $P_{\rm in}$ has been introduced into the SOA. The effect of an input pulse launched into the SOA is to deplete the carriers within the SOA. Carrier depletion is a fast SOA process, which instantaneously leads to a gain saturation in all signals present. This gain saturation is followed by a gain relaxation process, which is only limited by the SOA carrier relaxation time. The effect of this gain saturation and gain relaxation onto the cw signal is plotted in Fig. 3(a), where the dashed line shows the cw signal intensity with time. Yet, the dashed curve only shows the so-called XGM effect. As a matter of fact due to the Kramers-Kronig relations XGM goes along with a phase modulation (XPM) that leads to a chirped cw signal. The chirp may be given by

$$\Delta\nu(t) = \frac{1}{2\pi}\frac{\partial\left[\alpha\ln\left(\frac{G(t)}{G_0}\right)\right]}{\partial t} \tag{3}$$

where α is the linewidth enhancement factor, $G(t)$ is the saturated gain and G_0 is the unsaturated single pass SOA gain. We have measured the SOA chirp induced onto the cw signal and plotted it as a solid line in Fig. 3(a). In agreement with (3) one can see an initial red-chirp during the gain saturation phase followed by a blue chirp during the gain relaxation phase.

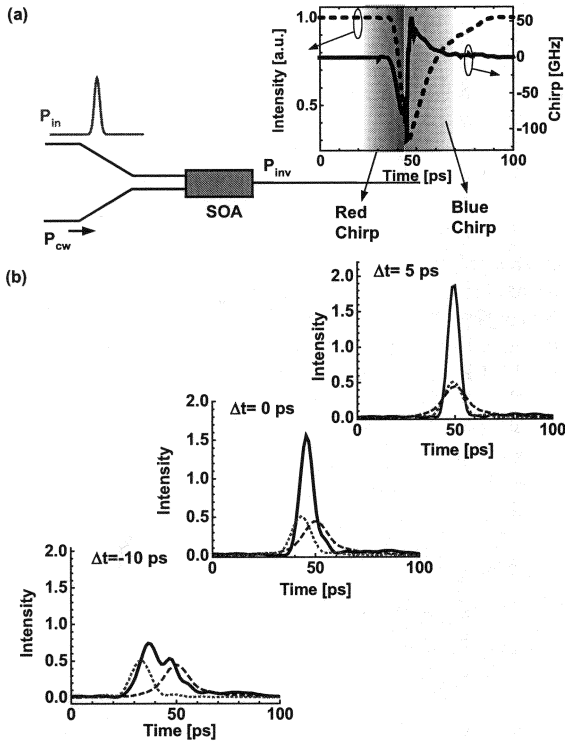

Fig. 3. (a) Intensity and chirp response of a cw signal passing through an SOA modulated by an input signal $P_{\rm in}$. The dashed line shows the cw signal with the inverted (with respect to input signal) response. The solid line shows the red shift followed by the blue shift frequency response of inverted signal. (b) Splitting off the red chirped (dotted) and blue chirped (dashed) spectral parts of the inverted signal and recombining them with time delays of -10, 0, and $+5$ ps produces a new signal (solid line). An almost ideal RZ signal with narrow Full-Width Half Maximum is obtained if the leading red-chirped spectrum is delayed by $+5$ ps with respect to the blue spectral slice.

The preceding discussion allows us to give the following interpretation of the ideal filter. In accordance with Fig. 2 we obtain an ideal wavelength converter by splitting off the red-chirped from the blue chirped part and by delaying the leading red-chirped part by approximately 5 ps with respect to the trailing blue chirped part before recombining them. The effect of splitting off and recombining the two spectral components while introducing different time delays are plotted in Fig. 3(b). The calculations show the converted signal (solid line) obtained when recombining the red chirped (dotted line) and the blue-chirped (dashed line) signals after time delays of $\Delta t = -10$ ps, 0 ps and $+5$ ps. And indeed, the best result is obtained when the red and blue-chirped signals have similar amplitudes and when the red chirped signal is delayed by $+5$ ps. What we have found is as a matter of fact a mode-beating configuration for the red and blue spectral components. It can be shown, that adapting the time delay between the pulses can modify the pulse shape.

At first sight it might look a little bit distressing, that we start with a series of "1" that is converted by means of SOA cross gain modulation into a series of "0" containing hardly any energy and which is then reformatted into a series of "1" containing energy. One might wonder where the energy of the "1" that are formed out of the "0" might come from. Yet, it needs to be noticed, that we are not using the inverted "0" signal level for forming the new pulses. Instead we are working with either the red chirped

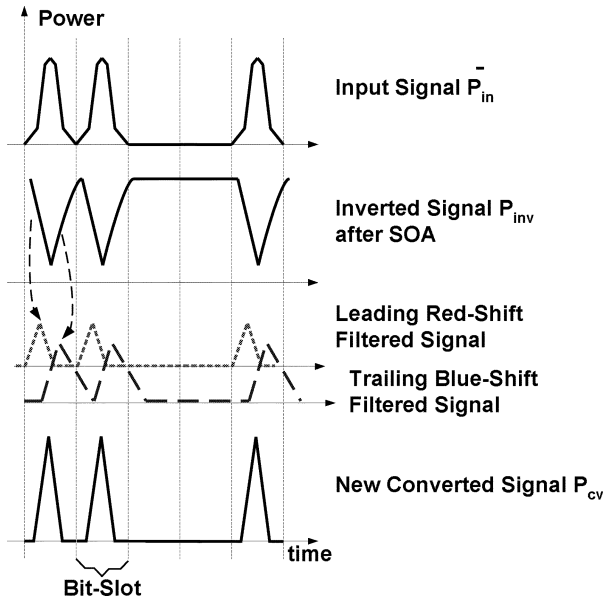

Fig. 4. Visualization of pulse form evolution and timing within the respective bit slots for idealized pulse shapes.

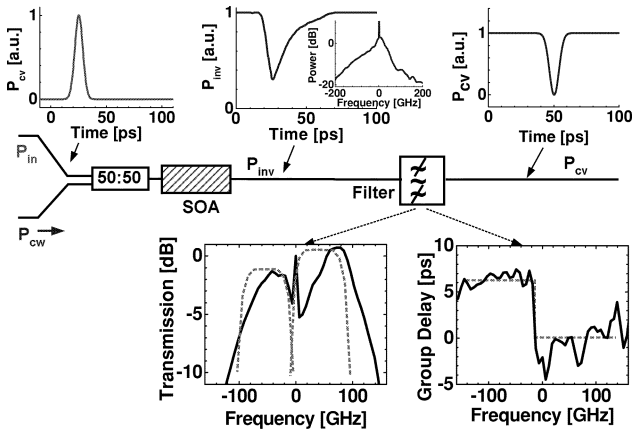

Fig. 5. Pulse shapes of input signal $P_{\rm in}$, inverted cw signal $P_{\rm inv}$ behind SOA and desired ideal inverted Gaussian shaped output pulse $P_{\rm cv}$. The ideal transmission and group delay frequency response of the PROF filter needed to perform the reformatting process is depicted at the bottom (solid lines). The dashed lines show a possible approximation for realizing such a filter.

signal induced beforehand generating the "0" or the blue chirped signal generated when the SOA relaxes back from the inverted state. Fig. 4 visualizes this concept by showing the input pulses, the inverted pulses, the split off red and blue chirped pulses and the converted signal as obtained by signal beating within the respective time slot.

B. RZ to NRZ All-Optical Wavelength Conversion

The appropriate filter for performing RZ to NRZ wavelength conversion is found by replacing the converted output signal with a NRZ signal. In a first attempt, we replace the Gaussian input signal from the RZ-to-RZ wavelength converter by a dark pulse with Gaussian shape, as drawn in Fig. 5. It is straightforward to show mathematically that the new filter performing RZ to inverted wavelength conversion is identical to the previous filter except for the region around $\Delta\nu(t) = 0$. In contrast to the previous scheme, we no longer cut out the cw frequency and it is

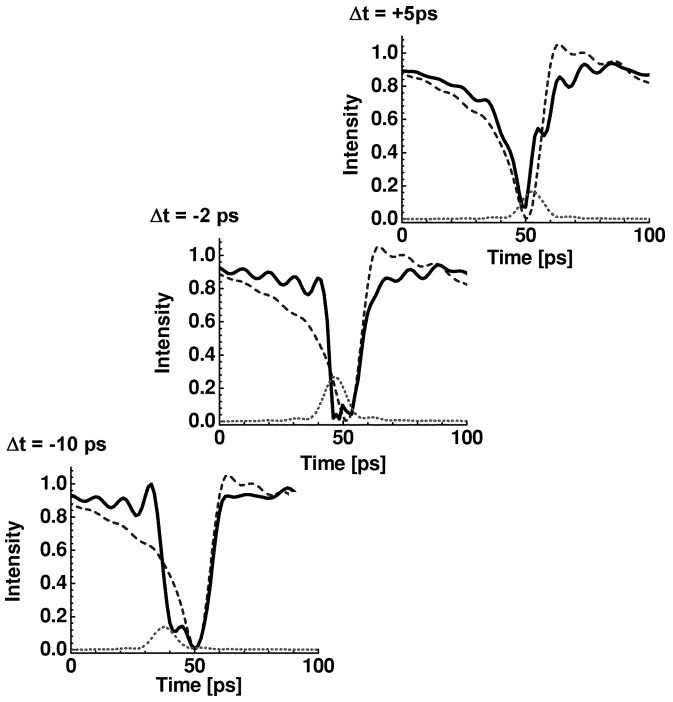

Fig. 6. Signal shape of the converted signal $P_{\rm cv}$ (solid line) at the output of a inverting PROF filter according to the recipe given in Fig. 5. While an almost Gaussian shape is obtained with $\Delta{\rm t} = +5$ ps delay, NRZ shapes of varying FWHM are obtained when the respective delays between red and blue chirped signals are in the range of -2 and -10 ps.

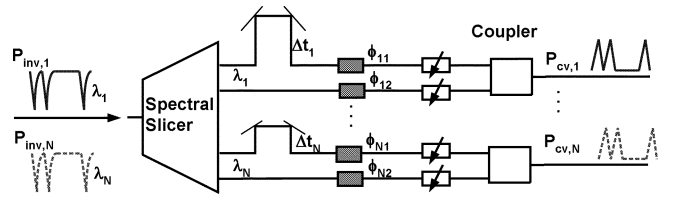

Fig. 7. Scheme of a pulse reformatting optical filter. The PROF filter comprises a spectral slicer, appropriate time delays for the different spectral components, phase shifters, attenuators and combiners.

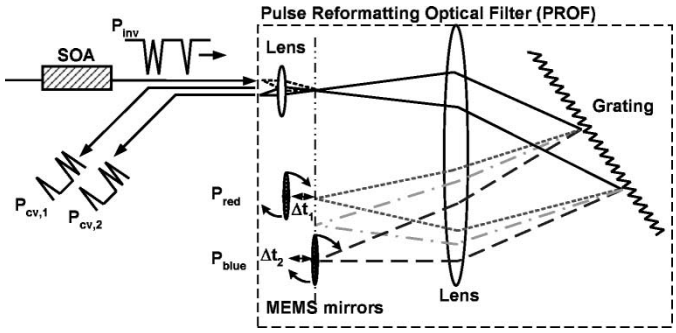

Fig. 8. Pulse reshaping optical filter (PROF) based on MEMS tilt-and-piston mirrors. The incoming signal is dispersed by the grating and two spectral components (red- and blue- shifted) are incident onto micro mirrors. The spectral components are reflected back to the grating and onto either of the two output fibers. The small section between the mirrors attenuates the cw component.

sufficient to cut the whole spectrum of the modulated cw signal into two spectral slices, Fig. 5 (bottom).

Adjusting the time delay between the two spectral slices changes the pulse shape We found that the dark Gaussian pulse converts into a NRZ shape if the blue component is delayed $\sim$10 ps relative to the red shift spectral component. Calculations of pulse shapes for different time delays are shown in Fig. 6. The NRZ shape with $\Delta{\rm t} = -10$ ps was obtained by attenuating the red-shift spectral component by 3 dB with respect to the blue-shift spectrum. While both the red and blue time responses have slowly varying slopes, we find sharp slopes for the pulse-reformatted pulses—for time delays of $\Delta{\rm t}$ between -2 and -10 ps.

Variations of this concept can be implemented. For instance, it would be relatively straight forward to add chirp to the different spectral slices and, thus, pre- or postcompensate dispersion while performing all-optical wavelength conversion.

III. Implementation of a Pulse Reformatting Optical Filter

For realizing a pulse reformatting optical filter, we need to spectrally slice the spectrum, introduce well-defined time delays onto the different spectral components, control the relative phases and recombine them with appropriate attenuations at the output. The general form of a PROF filter is depicted in Fig. 7.

Such a PROF filter could be implemented as a planar lightwave circuit filter, where the spectral slicer is a waveguide grating router (WGR) with phase-shifters and attenuators on the waveguides. The layout of the PROF filter in Fig. 7 shows that a single device can process multiple signals. This may make the scheme attractive for use in commercial systems.

Our implementation of a PROF filter was based on MEMS technology that not only allowed us to perform wavelength conversion but also to perform switching and adjustment of the time delay in order to change the output signal format. The setup with the MEMS switch device in a three-segment approximation to the ideal PROF filter is shown in Fig. 8. The device is similar to the MEMS switch array from [24]. The inverted signal that is to be filtered is launched through a lens onto a grating, which spectrally disperses the beam. and directs the spectral components toward two micro mirrors. The two mirrors have a 77-GHz 1-dB bandwidth, and a 89-GHz 3-dB passband characteristic., i.e., with respect to the cw frequency they span approximately 90 GHz of the red and 90 GHz of the blue shift spectrum. Between the two mirrors is a narrow nonreflecting gap. The MEMS mirrors can be actuated to provide rotational and piston motion. By applying tilt to either mirror, one changes the optical path length and thereby introduce group delays as well as attenuation for the respective spectral segments. The calculations from Fig. 3 show, that a 5 ps delay between the red and blue spectral segments with an additional 2 dB attenuation on the red side is needed for generating RZ→RZ wavelength conversion. The center spectral region is dominated by the cw signal that is to be attenuated in the nonreflecting gap between the two mirrors.

Switching is obtained by tilting the two mirrors simultaneously so that the light from the two mirrors combine in either the first $(P_{\rm cv,1})$ or the second $(P_{\rm cv,2})$ output fiber. Since the switch fabric was equipped with mirrors all across the C-band, future versions may be used in a WDM environment populated every 200 GHz.

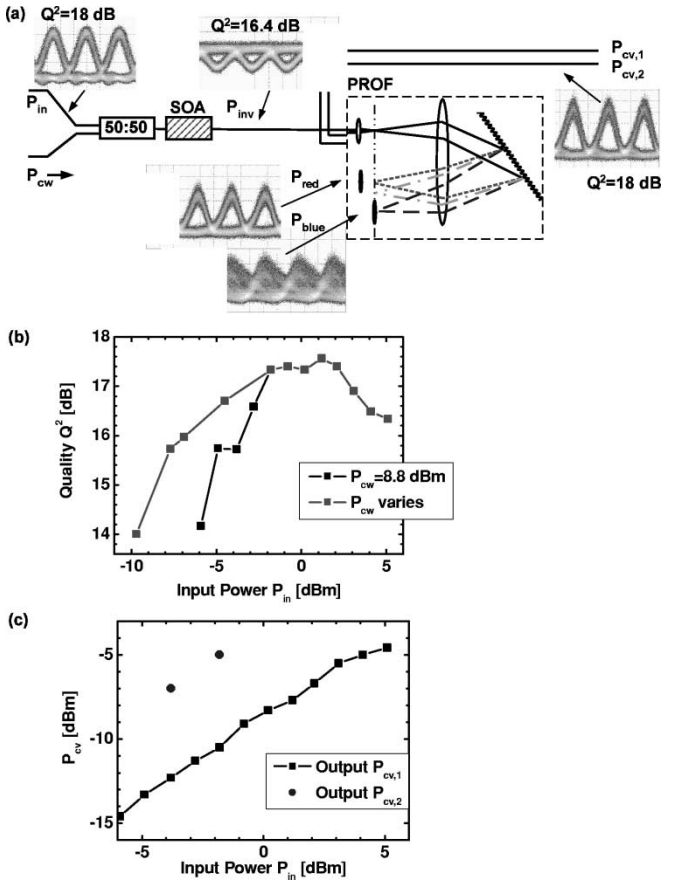

Fig. 9. (a) Eye diagram of input signal $\mathrm{P_{in}}$, inverted signal $\mathrm{P_{inv}}$ after SOA and converted signal $\mathrm{P_{cv}}$. The eye diagrams of the signals from the respective mirrors are shown at the bottom. The eye diagram of the converted signal $\mathrm{P_{cv}}$ has excellent quality and has a visibly shorter FWHM than the FWHM of the input signal. (b) Signal qualities of the converted signal for various input-powers without adaptation of filter parameters (triangles) and with adaptation of the cw input power levels (squares) (c).

IV. Experimental Setup and Results

To test the concept we generated 40 Gb/s RZ data signals with a 33% duty cycle ($\lambda_{\mathrm{in}} = 1559\ \mathrm{nm}$). The 40 Gb/s signal was obtained by electrically multiplexing four 10 Gb/s channels with a pseudorandom bit sequence (PRBS) of length $2^{31} - 1$. The wavelength of the cw source was 1553 nm. A 2-mm long bulk SOA (700 mA applied current) provided the necessary nonlinearities for switching. An electroabsorption modulator was used to demultiplex the optical signal from 40 to 10 Gb/s before guiding the signal into a receiver and evaluating the signal in a bit error rate tester (BERT).

We first discuss the experiments on generating noninverted and then the experiments on generating bit-inverted wavelength conversion.

For performing noninverted RZ→RZ signal wavelength conversion, the delay between the mirrors and the attenuation was set to 5 ps as discussed earlier. Eye diagrams from this experiment are given in Fig. 9(a). Signal Q^2-factors were measured with a BERT. We found values of $\mathrm{Q}^2 = 18$, 16.4 and 18 dB for the input data signal, the inverted signal between the SOA and the PROF and the converted signal, respectively. The eye of the wavelength-converted signal is not only clear and open but also is the FWHM of the converted signal visibly shorter than the FWHM of the input signal. This pulse-width regeneration is a result of the signal beating between the blue and red spectral components. The eye diagrams were taken with input signal powers of -1.5 dBm and a cw signal power of 2.3 dBm. All powers are measured in the fiber behind the 3-dB coupler before the SOA.

Signal Q^2-factors for various input-powers are given in Fig. 9(b). An input-power dynamic range of 10 dB (with Q^2 better than 15.6 dB) is found when the cw power is kept constant at 8.8 dBm (triangles). If we allow for adjustment of the cw signal power with changing input signal power, the input dynamic range greatly increases and wavelength conversion with bit error rates below $1 \cdot 10^{-9}$ is obtained with as little as -8.5 dBm (squares).

While signal quality below 16 dB can be measured exactly, signal quality better than 16 dB are estimated by extrapolation. Such extrapolations are based on assumptions for the noise distributions. Yet, as it is not clear on what noise distribution we have after an all-optical wavelength conversion operation it may be that the extrapolated values differ based on the method used. However, the quantitative values given here are still indicative for the quality of the signal and are in agreement with bit-error rate sensitivity measurements. All of our Q^2 values are interpolated from the inverse complementary error function [25].

The conversion efficiency for varying input power levels when mapping the signal onto output 1 or output 2 are depicted in Fig. 9(c). The conversion efficiency onto output 2 is higher due to reduced losses within the MEMS setup for the different outputs. We have performed only few measurements with output channel 2. Yet these few measurements follow the trend of channel 1 as one would expect.

For performing bit-inverted wavelength conversion we choose the PROF filter as derived in Fig. 6. NRZ bit-inverted conversion is obtained when the blue chirped spectral components are delayed by approximately 10 ps with respect to the red-chirped spectral components and when the cw spectral component passes almost unfiltered. With our MEMS based device we only needed to reconfigure the mirrors positions and apply other angles in order to change the format.

Signal qualities of the bit-inverted experiment are shown in the plot of Fig. 10(a). We find that bit-inverted wavelength conversion can be performed with as little as -17.5 dBm (i.e., 0.45 fJ per pulse in the fiber before the SOA). To the best of our knowledge this is an order of magnitude improvement over what has been reported so far and competes with state-of-the-art optical-electrical receiver sensitivities [26]. We further measure an input dynamic range that exceeds 20 dB when the cw signal is adapted to the power of the input signal and an input dynamic range of approximately 11 dB when the cw signal power is fixed to -5.5 dBm. It is important to note, that the PROF is not necessary for bit-inverted all-optical wavelength conversion. However, without the PROF, the Q^2 is degraded. This is seen from the eye diagram in Fig. 10, where an input signal at -9.0 dBm is launched into the SOA—without PROF (bottom eye diagram) and with PROF (top eye diagram). Not only is the eye much wider and less noisy but also is the measured signal quality much better with the PROF.

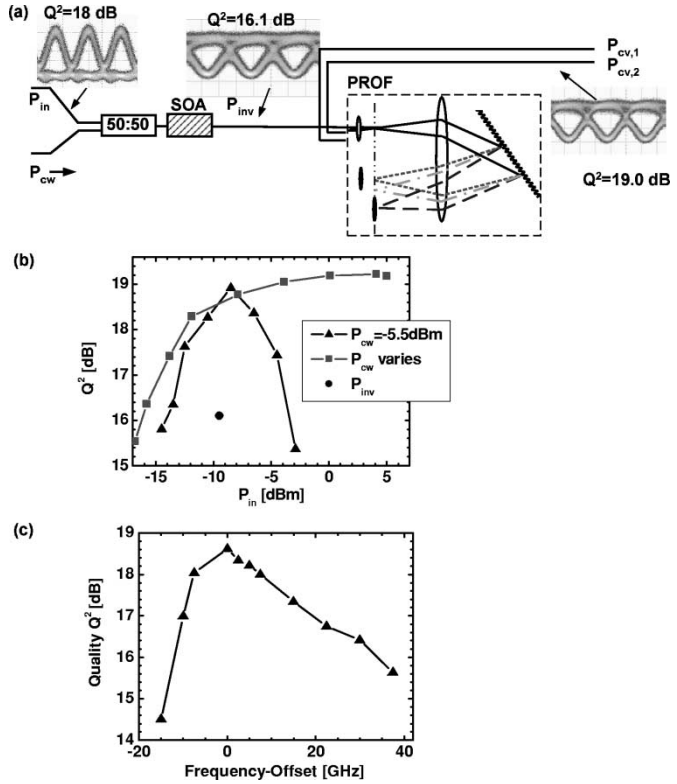

Fig. 10. (a) and (b) Signal quality versus input-power of bit-inverted wavelength conversion when cw power is constant (triangles) and when cw power is adapted with respect to input signal powers (squares). The eye diagrams are for an input-signal of -9 dBm signal power. (c) Tolerance to frequency offsets of the cw frequency with respect to the filter.

Tolerance of the PROF scheme to cw frequency deviations was also tested. Fig. 10(c) shows signal qualities measured for various cw frequency offsets. Deviations of 15 and 40 GHz from the optimum frequency into the red and blue spectrum can be tolerated for signal qualities better than 15.6 dB, i.e. with bit error rates better than 1×10^{-9}.

V. Conclusion

We have demonstrated a new method of optical filtering to achieve all-optical wavelength conversion of 40 Gb/s signals with output Q^2-factors exceeding 18 dB. The method also enabled low input-power operation with 40 Gb/s input sensitivities of -17.5 dBm and large input power dynamic ranges of 11 to 20 dB. A MEMS-based filter implementation has allowed us to perform simultaneous wavelength conversion, switching and format conversion.

Acknowledgment

The authors would like to thank J. L. Pleumeekers for the contributions and R. J. Essiambre, M. Duelk, C. K. Madsen, D. T. Neilson, and R. M. Jopson for helpful discussions.

References

[1] S. Nakamura, Y. Ueno, and K. Tajima, , Quebec, QC, Canada, July 2000, paper pd. 4.

[2] J. Leuthold, C. H. Joyner, B. Mikkelsen, G. Raybon, J. L. Pleumeekers, B. I. Miller, K. Dreyer, and C. A. Burrus, "100 Gbit/s all-optical wavelength conversion with integrated SOA delayed-interference configuration," *Elec. Lett.*, vol. 36, no. 13, pp. 1129–1130, June 2000.

[3] W. Idler, M. Schilling, K. Daub, D. Baums, U. Korner, E. Lach, E. Laube, and K. Wunstel, "Signal quality and BER performance improvement by wavelength conversion with an integrated three-port Mach-Zehnder interferometer," *Elect. Lett.*, vol. 31, no. 6, pp. 454–455, Mar. 1995.

[4] J. De Merlier, G. Morthier, T. V. Caenegem, R. Baets, I. Moerman, and P. Van Daele, "Experimental demonstration of 15 dB extinction ratio improvement in a new 2R optical regenerator based on an MMI-SOA," in *Proc. Eur. Conf. Opt. Comm. (ECOC'01)*, Amsterdam, The Netherlands, Sept. 2001, pp. 574–576.

[5] D. Wolfson, A. Kloch, T. Fjelde, C. Janz, B. Dagens, and M. Renaud, "40-Gb/s all-optical wavelength conversion, regeneration, and demultiplexing in an SOA-based all-active Mach-Zehnder interferometer," *IEEE Photon. Technol. Lett.*, vol. 12, pp. 332–334, Mar. 2000.

[6] J.-Y. Emery, M. Picq, F. Poingt, F. Gaborit, R. Brenot, M. Renaud, B. Lavigne, and A. Dupas, "Optimized 2-R all-optical regenerator with low polarization sensitivity penalty ($<$1 dB) for optical networking applications," presented at the OFC'2001, vol. 1, Anaheim, CA, paper MB4.

[7] J. Leuthold and M. Kauer, "Power equalization and signal regeneration with delay interferometer all-optical wavelength converters," *Elect. Lett.*, vol. 38, no. 24, pp. 1567–1569, Nov. 2002.

[8] J. Leuthold, R. Ryf, and D. Maywar, "Novel all-optical wavelength converter in an add/drop multiplexing network demonstrating transmission over 42 nodes and 16'800 km," presented at the Proc. LEOS'2002 Annu. Meet., Glasgow, U.K., Nov. 2002, paper PD 1.3.

[9] B. Lavigne *et al.*, "Cascade of 100 optical 3R regenerators at 40 Gbit/s based on all-active Mach-Zehnder interferometers," in *Proc. ECOC'01*, vol. 3, Sept. 2001, pp. 290–293.

[10] J. Leuthold, G. Raybon, Y. Su, R. Essiambre, S. Cabot, J. Jaques, and M. Kauer, "40 Gb/s transmission and cascaded all-optical wavelength conversion over one million kilometers," *Elect. Lett.*, vol. 38, no. 16, pp. 890–892, Aug. 2002.

[11] M. Duelk, S.St. Fischer, E. Gamper, W. Vogt, E. Gini, H. Melchior, W. Hunziker, H. N. Poulsen, A. T. Clausen, A. Buxens, and P. Jeppesen, "Efficient regenerative wavelength conversion at 10 Gbit/s over C- and L-band using a Mach-Zehnder interferometer with monolithically integrated semiconductor optical amplifier," *Elect. Lett.*, vol. 36, no. 3, pp. 241–243, Feb. 2001.

[12] C. Joergensen, T. Duurhus, B. Mikkelsen, and K. E. Stubkjaer, "Wavelength conversion at 2.5 Gb/s using a MZI with SOA's," in *Proc. OAA'1993*, Yokahama, Japan, July 1993, pp. 154–157.

[13] K. Tajima, "All-optical switch with switch-off time unrestricted by carrier lifetime," *Jpn. J. Appl. Phys.*, vol. 32, no. 12A, pp. L1746–L1749, Dec. 1993.

[14] J. P. Sokoloff, P. R. Prucnal, I. Glesk, and M. Kane, "A terahertz optical symmetric demultiplexer (TOAD)," *IEEE Photon. Technol. Lett.*, vol. 5, pp. 787–790, July 1993.

[15] K. Tajima, S. Nakamura, and Y. Sugimoto, "Ultrafast polarization-discriminating Mach-Zehnder all-optical switch," *Appl. Phys. Lett*, vol. 67, no. 25, Dec. 1995.

[16] K. L. Hall and K. A. Rauschenbach, "100-Gbit logic," *Opt. Lett.*, vol. 23, no. 16, pp. 1271–1273, Aug. 1998.

[17] Y. Ueno, S. Nakamura, K. Tajima, and S. Kitamura, "3.8-THz wavelength conversion of picosecond pulses using a semiconductor delayed-interference signal-wavelength converter (DISC)," *IEEE Photon. Technol. Lett.*, vol. 10, pp. 346–349, Mar. 1998.

[18] J. Leuthold, C. H. Joyner, B. Mikkelsen, G. Raybon, J. L. Pleumeekers, B. I. Miller, K. Dreyer, and C. A. Burrus, "Compact and fully packaged wavelength converter with integrated delay interferometer for 40 Gbit-s RZ signals," presented at the Proc. of Optical Fiber Communication Conference (OFC'2000), Baltimore, MD, Mar. 2000, pd. 17.

[19] J. Leuthold, B. Mikkelsen, R. E. Behringer, G. Raybon, C. H. Joyner, and P. A. Besse, "Novel 3R regenerator based on semiconductor optical amplifier delayed-interference configuration," *IEEE Photon. Technol. Lett.*, vol. 13, pp. 860–862, Aug. 2001.

[20] K. E. Stubkjaer, T. Durhuus, B. Mikkelsen, C. Joergensen, R. J. Pedersen, C. Braagaard, M. Vaa, S. L. Danielsen, P. Doussiere, G. Garabedian, C. Graver, A. Jourdan, J. Jacquet, D. Leclerc, M. Erman, and M. Klenk, "Optical wavelength converters," in *Proc. Eur. Conf. Opt. Comm. ECOC'94*, vol. 2, Firence, Italy, 1994, pp. 635–642.

[21] J. Leuthold, B. Mikkelsen, R. E. Behringer, G. Raybon, C. H. Joyner, and P. A. Besse, "Novel 3R regenerator based on semiconductor optical amplifier delayed-interference configuration," *IEEE Photon. Technol. Lett.*, vol. 13, pp. 860–862, Aug. 2001.

[22] J. Leuthold, B. Mikkelsen, G. Raybon, C. H. Joyner, J. L. Pleumeekers, B. I. Miller, K. Dreyer, and R. Behringer, "All-optical wavelength conversion between 10 and 100 Gb/s with SOA delayed-interference configuration," *Optical Quantum Electron.*, vol. 33, no. 7–10, pp. 939–952, July 2001.

[23] C. K. Madsen and J. H. Zhao, *Optical Filter Design and Analysis*. New York: Wiley, 1999.

[24] D. M. Marom, D. T. Neilson, D. S. Greywall, N. R. Basavanhally, P. R. Kolodner, Y. L. Low, F. Pardo, C. A. Bolle, S. Chandrasekhar, L. Buhl, C. R. Giles, S.-H. Oh, C. S. Pai, K. Werder, H. T. Soh, G. R. Bogard, E. Ferry, F. P. Klemens, K. Teffeau, J. F. Miner, S. Rogers, H. E. Bower, R. C. Keller, and W. Manfield, "Wavelength-selective 1×4 switch for 128 WDM channels at 50 GHz spacing," presented at the Proc. Optical Fiber Communication Conf., 2002, pd. FB7.

[25] N. S. Bergano, F. W. Kerfoot, and C. R. Davidson, "Margin measurements in optical amplifier systems," *IEEE Photon. Technol. Lett.*, vol. 5, pp. 304–306, Mar. 1993.

[26] B. Mason, J. M. Geary, J. M. Freund, A. Ougazzaden, C. Lentz, K. Glogovsky, G. Przybylek, L. Peticolas, F. Walters, L. Reynolds, J. Boardman, T. Kercher, M. Rader, D. Monroe, and L. Ketelsen, "40 Gb/s photonic integrated receiver with -17 dBm sensitivity," presented at the Optical Fiber Communication Conf. Exhibit, Mar. 17–22, 2002, paper FB10.

Juerg Leuthold (S'95–A'98–M'99) was born in St. Gallen, Switzerland, in 1966. He received the diploma, degree in physics, and the Ph.D. degree from the Swiss Federal Institute of Technology (ETH), Zurich, Switzerland, in 1991 and 1998, respectively.

In 1992, he joined the Institute of Quantum Electronics of the Swiss Federal Institute of Technology, where he worked in the field of integrated optics. Since 1999, he has been affiliated with Bell Labs, Lucent Technologies, Holmdel, NJ, where he is continuing research on III/V semiconductors for high-speed telecommunication applications and performing system experiments with high-speed components.

Dan M. Marom received the B.Sc. degree in mechanical engineering and the M.Sc. degree in electrical engineering, both from Tel-Aviv University, Tel-Aviv, Israel, in 1989 and 1995, respectively, and the Ph.D. from University of California, San Diego (UCSD), in 2000.

In his doctoral dissertation, he investigated femtosecond-rate optical signal processing with applications in ultrafast communications. From 1996 through 2000, he was a Fannie and John Hertz Foundation Graduate Fellow at UCSD. In 2000, he joined the Advanced Photonics Research Department at Bell Laboratories, Lucent Technologies, where he is working on novel MEMS based switching solutions using MEMS technology for optical communications

Dr. Marom received the IEEE Lasers and Electro-Optics Society Best Student Paper Award in 1999 for his work describing instantaneous time reversal of complex amplitude ultrafast waveforms.

Steven Cabot was born in Plainfield, NJ, in 1966. He studied electrical engineering at Union County College, Elizabeth, NJ, and at the New Jersey Institute of Technology, Newark.

He first started working for Bell Labs, Holmdel, NJ, in 1989 in Federal Systems building undersea optical assemblies. He moved to research in 1993, where he worked on erbium fiber characterization and EDFA assemblies. In 1999, he joined the Specialty Fiber Business Unit working on high power components and assemblies. In 2001, he joined Onetta working on novel EDFA architectures in the forward looking group. He then rejoined Bell Labs in 2002 in the Government Communication Lab.

James J. Jaques was born in Raleigh, NC, in 1967. He received the B.S. degree in physics from Virginia Tech, Blacksburg, VA, in 1989, and the M.S. and Ph.D. degrees in particle physics from the University of Notre Dame, Notre Dame, IN, in 1992 and 1997, respectively, where he helped develop a particle tracking system using organically doped polymer optical fibers.

In 1998, he joined Lucent Technologies, Bell Laboratories, Holmdel, NJ, as a Member of the Technical Staff. He currently works on novel SOA-based integrated components and high power optical fiber amplifiers.

Roland Ryf received the B.S. degree in engineering from the Interstate University of Applied Sciences of Technology Buchs, Switzerland, in 1990, and the M.S. and Ph.D. degrees in physics from the Swiss Federal Institute of Technology, Zurich, Switzerland, in 1995 and 200, respectively.

Since May 2000, he has been with the Photonic Subsystems Department, Bell Labs, Lucent technologies, Holmdel, NJ, where he is focusing on the subsystem design and prototyping of large port count optical MEMs-based switches and demonstration of their of applications in transparent optical networks.

C. Randy Giles received the B.Sc. and MSc. degrees in physics from the University of Victoria, BC, Canada, in 1976 and 1978, respectively, and the Ph.D. degree in electrical engineering from the University of Alberta, Canada, in 1983.

From 1983 to 1986, he researched semiconductor lasers and technology for gigabit/s optical transport systems as a Member of the Scientific Staff at Bell Northern Research. In 1986, Dr. Giles joined Bell Laboratories, Holmdel, NJ, and is currently the Director of Advanced Photonics Research. His research centers on optical network applications of new technologies, including MEMS, high-speed optical signal conditioners, and active optical network monitors. His department researches in the areas of wavelength-selective switching, photonic structures, ultrafast wavelength conversion and signal regeneration, ultrafast pulse and data stream characterization, and advanced optical transport.

Dr. Giles is a Fellow of the Optical Society of America (OSA) and a Bell Laboratories Fellow.